

## COMMUNICATION

# The Activity of siRNA in Mammalian Cells is Related to the Kinetics of siRNA-target Recognition *In Vitro*: Mechanistic Implications

Winfried Wünsche and Georg Sczakiel\*

Universität zu Lübeck, Institut  
für Molekulare Medizin  
Ratzeburger Allee 160, D-23538  
Lübeck, Germany

The specificity of siRNA-mediated suppression of gene expression involves base–base recognition between siRNA and its single-stranded RNA target. We investigated the kinetics of this process *in vitro* by using full-length ICAM-1 target RNA and biologically active and inactive ICAM-1-directed siRNA, respectively. To mimic the situation in living cells we used the well-characterised facilitator of RNA–RNA annealing and strand exchange cetyltrimethylammonium bromide, which increases strongly the kinetics of RNA–RNA interactions at conditions that do not affect RNA structure nor the presumed structure–function relationship. For the biologically active siRNA si2B, we find faster binding, i.e. recognition of the target and a slower backward reaction when compared with the biologically inactive siRNA si1. This is reflected by an approximately 400-fold more favorable equilibrium constant of si2B. Kinetic evidence favors an associative mechanism of recognition of the target strand by the double-stranded siRNA. The minimal model for siRNA-target recognition described here is consistent with the high biological activity of si2B only if one assumes a step subsequent to target recognition, which might be degradation of the target RNA when complexed with the antisense strand of siRNA or when considering rapid destruction of the released sense strand of siRNA.

© 2004 Elsevier Ltd. All rights reserved.

**Keywords:** associative mechanism; facilitator; RNA–RNA recognition; siRNA; RISC

\*Corresponding author

The mechanism by which siRNA recognizes and binds to its target RNA in mammalian cells and suppresses target gene expression post-transcriptionally is assumed to include base-specific recognition. Whether this recognition involves the double-stranded siRNA in living cells or, subsequent to its dissociation, the single-stranded antisense strand is open though a dissociation step preceding siRNA-target RNA interaction is consistent with a number of *in vitro* studies.<sup>1</sup> For example, an ATP-dependent step subsequent to the function of DICER<sup>2</sup> and prior to the formation of a siRNA-activated RNA-induced silencing complex (RISC) has been suggested,<sup>3</sup> and the observation

that RISC may contain only one of the two strands of siRNA<sup>4</sup> is compatible with this view. Further, an asymmetric internal thermal stability of functional siRNA but not of non-active ones indicated that a relatively instable 5'-end of the antisense strand is related to increased biological activity by providing an intrinsic information of siRNA for strand-specificity of the activated RISC.<sup>1,5</sup> In living cells, however, the order of interactions leading to the specificity of target recognition by siRNA might be more complex and partly different from model reactions *in vitro*.

It is reasonable to assume that RNA–RNA interactions in living cells are facilitated by cellular metabolites and proteins that may interact with siRNA and target RNA in addition to proteins known to be involved specifically in siRNA mechanisms. Known facilitators of RNA–RNA interactions comprise a number of cellular proteins, such as hnRNP proteins.<sup>6,7</sup> As a model compound

Abbreviations used: siRNA, silencing RNA; CTAB, cetyltrimethylammonium bromide; s, sense; as, antisense; T, target; RISC, RNA-induced silencing complex.

E-mail address of the corresponding author:  
sczakiel@imm.uni-luebeck.de

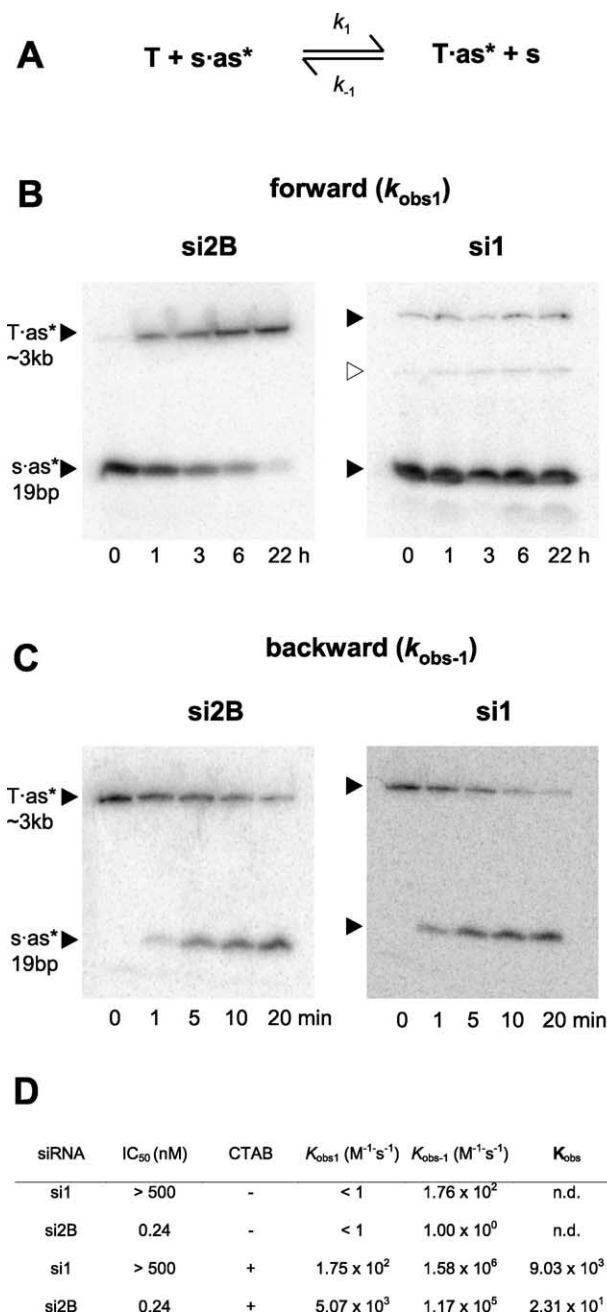


**Figure 1.** Kinetics of the strand exchange between siRNA and ICAM-1 target RNA. (A) The simplified reaction scheme. (B) A representative gel analyses of the forward strand-exchange reaction for si2B and si1, respectively in the presence of 10 mM CTAB; (C) the corresponding backward reactions. (D) A summary of the rate constants and equilibrium constants in the absence or presence of CTAB. Abbreviations and symbols:  $k_{obs1}$ , observed forward reaction rate constant;  $k_{obs-1}$ , observed backward reaction rate constant;  $K_{obs}$ , observed equilibrium constant; filled arrowheads indicate the double-stranded RNA complexes T·as (~3 kb) and s·as (19 bp), respectively; the open arrowhead indicates a contaminating product. The asterisk (\*) indicates that the antisense strand of si2B and si1, respectively, has been <sup>32</sup>P-labelled in the reactions shown in B and C. Cloning of the plasmid serving as template for *in vitro* transcription of ICAM-1 target RNA: total poly(A)<sup>+</sup> RNA was prepared from ECV304 cells that had served as the biological test system in earlier studies on siRNA.<sup>12</sup> After reverse transcription with Superscript II (Invitrogen, Karlsruhe, Germany) and random primer (Invitrogen), cDNA was amplified with forward primer (5'-CCC AGT CGA CGC TGA GCT CC-3') and reverse primer (5'-GAG AAA GCT TTA TTA ACT AAC AC-3') to generate a product of 2974 bp (positions 5–2979 of ICAM-1 cDNA, AC: J03232). This fragment was inserted into plasmid pCR2.1 (Invitrogen, Karlsruhe, Germany). For *in vitro* transcription the ICAM-DNA was sub-cloned into the EcoRI-site of pGEM3Z. ICAM-1-

specific RNA was transcribed *in vitro* with phage T7 RNA polymerase from SspI/HindIII-linearized plasmid pGEM3Z-ICAM-1. Briefly, a 100  $\mu$ l reaction mixture contained 2  $\mu$ g of template, 2 mM NTPs, 80 units of RNase inhibitor (MBI, Fermentas, St Leon-Roth), 400 units of T7 RNA polymerase (MBI, Fermentas, St Leon-Roth) in Polymerase-Puffer (MBI, Fermentas, St Leon-Roth). After incubation for two hours at 37 °C, template DNA was treated with 20 units of DNaseI (Invitrogen, Karlsruhe, Germany). The ICAM-1 transcript was extracted with phenol (pH 4.5–5.0), extracted with chloroform, purified by gel-filtration *via* a Nick-column (Amersham Biosciences, Uppsala, Schweden), and precipitated by adding 10% (v/v) 3 M sodium acetate (pH 5.2) and 2.5 volumes of 100% ethanol. For re-folding of target RNA, a solution containing 100 nM ICAM-1 RNA in 20 mM Tris-HCl (pH 7.5), 100 mM NaCl was heated at 65 °C for ten minutes and then cooled slowly to room temperature. Oligoribonucleotides (10 pmol, supplied by Eurogentec, Seraing, Belgium; quality assured by PAGE-purification and characterization by mass spectrometry) were labeled with 50  $\mu$ Ci of [ $\gamma$ -<sup>32</sup>P]ATP (NEN, Boston, USA), ten units of phage T4 polynucleotide kinase (MBI Fermentas, St Leon-Rot, Germany) in Reaction Buffer (MBI Fermentas) in a total volume of 20  $\mu$ l, incubated at 37 °C for 30 minutes, and purified *via* gel-filtration. Equimolar amounts of complementary oligoribonucleotides were incubated in 20 mM Tris-HCl (pH 7.5), 100 mM NaCl at 95 °C for five minutes followed by incubation for one hour at 37 °C. The annealing products were analyzed by PAGE (15% (w/v) acrylamide) under semi-denaturing conditions (4 M urea, 4 °C). For determining forward reaction rates, a typical reaction was performed in a volume of 50  $\mu$ l containing between 5 nM and 80 nM ICAM-1 RNA, 0.5 nM siRNA containing a <sup>32</sup>P-labelled antisense strand, 10 mM CTAB (Sigma, Deisenhofen, Germany), 20 mM Tris-HCl (pH 7.5), 100 mM NaCl at a temperature of 50 °C. Since the reaction time was almost one day, we controlled for degradation. Similar mixtures lacking unlabelled ICAM-1 RNA were incubated under the same conditions. Aliquots

**Table 1.** Relationship between the biological activity of ICAM-1-directed siRNAs and the kinetics of strand exchange with a long-chain ICAM-1 target RNA *in vitro* in the presence of the facilitator of RNA–RNA recognition CTAB

Name	IC <sub>50</sub> (nM) <sup>a</sup>	$k_{\text{obs}1}$ (M <sup>-1</sup> s <sup>-1</sup> )	$k_{\text{obs}-1}$ (M <sup>-1</sup> s <sup>-1</sup> )	$K_{\text{obs}}$	Nucleotide sequence <sup>b</sup>	$T_m$ (°C)	$\Delta G$ (kcal/mol)	
							5'-end	3'-end <sup>c</sup>
si1	> 500	$1.75 \times 10^2$	$1.58 \times 10^6$	$9.00 \times 10^3$	5'-ACCGUGAAUGUGCUCUCCCTt-3' 3'-ttUGGCACUUACACGAGAGGG-5'	69.5	-10.3	-11.1
si424	100	<10 <sup>2</sup>	$1.49 \times 10^5$	> $1.49 \times 10^3$	5'-UCUUGGCAGCCAGUGGGCAAGtt-3' 3'-ttAGAACCUGCGUCACCCGUUC-5'	76.4	-7.8	-9.0
si429	80	<10 <sup>2</sup>	$8.80 \times 10^4$	> $8.80 \times 10^2$	5'-GCAGCCAGUGGGCAAGAACCt-3' 3'-ttCGUCGGUCACCCGUUCUUGGA-5'	76.8	-11.7	-8.7
si2B	0.24	$5.07 \times 10^3$	$1.17 \times 10^5$	$2.40 \times 10^1$	5'-GCCUCAGCAGUACCCUUA-3' 3'-ttCGGAGUCGUGCAUGGAGAU-5'	69.9	-11.6	-7.8
si843	3	$4.80 \times 10^2$	$8.60 \times 10^4$	$1.79 \times 10^2$	5'-AGUCACCUAUGGCAACGACU-3' 3'-ttUCAGUGGAUACCCGUUCGUGAG-5'	70.2	-9.1	-9.6
si860	2	$1.70 \times 10^3$	$7.40 \times 10^3$	$4.35 \times 10^0$	5'-ACUCCUUCUCGGCCAAGCCU-3' 3'-ttUGAGGAAGAGCCGGUUCGGGA-5'	77.4	-10.2	-12.3
si1546	4	$1.76 \times 10^3$	$1.43 \times 10^5$	$8.13 \times 10^1$	5'-GGCCUCAGCAGUACCCUUA-3' 3'-ttCCGGAGUCGUGCAUGGAGAU-5'	73.7	-12.3	-7.0
si1637	1	$2.57 \times 10^3$	$1.18 \times 10^5$	$4.59 \times 10^1$	5'-CACAGCCAGCCUCCUGAA-3' 3'-ttGUGUUCGGUGCGGAGGACUU-5'	75.5	-7.9	-7.9

<sup>a</sup> Apparent IC<sub>50</sub> values of the siRNA-mediated inhibition of ICAM-1 in ECV 304 cells was measured as described.<sup>12</sup>

<sup>b</sup> The upper strand represents the "sense" orientation, the lower strand has "antisense" polarity with respect to the ICAM-1 target RNA.

<sup>c</sup> The  $\Delta G$  values are calculated for the terminal five pairs at the 5'-end or the 3'-end of the sense strand of siRNA using the program Oligo 6.0 (<http://www.oligo.net/>).

of such proteins, one considers quarternary ammonium salts such as cetyltrimethylammonium bromide (CTAB) which, in principle, share the functional domains of the facilitators hnRNP protein A1.<sup>8</sup> Many facilitators increase the annealing of complementary RNA by two to three orders of magnitude. Remarkably, the strand exchange between double-stranded and single-stranded RNA may be increased by even 10<sup>4</sup>-fold and higher.<sup>9</sup> This great increase of the kinetics of RNA–RNA strand displacement suggests that this process can be regulated tightly by cellular factors in a living cell. It is thus reasonable to investigate facilitated interactions between siRNA and target RNA that might be relevant for the action of siRNA *in vivo*.<sup>10</sup> It is noteworthy that some very potent facilitators such as p53 and CTAB increase the kinetics of RNA–RNA recognition substantially without measurably affecting RNA structure or the mode of intermolecular interactions of RNA,<sup>7,11</sup> suggesting that RNA–RNA interactions are promoted in an enzyme-like fashion, implying the lack

of influence of facilitators on the structure–function relationship.

Here, we attempt to introduce a biochemical parameter that links characteristics of siRNA–target RNA recognition *in vitro* to the biological activity of siRNA in living cells. We investigated the kinetics of the interactions between the biologically highly active ICAM-1-directed siRNA si2B<sup>12</sup> and the inactive siRNA si1 with target RNA *in vitro*. As a well-characterized and robust facilitator, we used CTAB, which is known to facilitate RNA–RNA annealing,<sup>8,11</sup> as well as RNA–RNA strand exchange *in vitro*.<sup>9</sup> When looking at the mode of action of siRNA, a kinetic approach seems to be helpful for several reasons: measuring the kinetics of the interactions between siRNA and its target might allow one to derive a minimal mechanistic model of siRNA-mediated suppression of its target that can serve as a basis for falsification or further verification and refinement. Further, looking at the kinetics does not require knowledge of RNA structures. Analogous approaches have been

(8  $\mu$ l) of the reaction mixtures were withdrawn at certain time-points, 8  $\mu$ l of stop buffer was added (20 mM Tris–HCl (pH 7.5), 10 mM EDTA, 2% (w/v) SDS, 8 M urea), and samples were frozen in liquid nitrogen. Samples were analyzed by PAGE (15% acrylamide) containing 4 M urea at 10 V/cm and a temperature of 4 °C, which resolves minor folding but does not denature siRNA or the heteroduplex RNA. Backward reactions were started with a pre-annealed complex of target RNA (2 nM) and <sup>32</sup>P-labelled antisense strands of the siRNAs (0.5 nM) in a total volume of 50  $\mu$ l containing 20 mM Tris–HCl (pH 7.5), 100 mM NaCl, and with or without 10 mM CTAB at a temperature of 50 °C or 60 °C, respectively. Reactions were started by adding the sense strand of siRNA at a final concentration of 2.5–80 nM (in the presence of CTAB) or at 4.5  $\mu$ M in the absence of CTAB. Samples were withdrawn, the reaction was stopped by the buffer described above, frozen in liquid nitrogen, and analyzed by PAGE as described above. To visualize and to quantify polyacrylamide gels containing reaction mixtures from forward or backward reactions, we used a Phospho-Imager (Amersham Pharmacia Biotech, Freiburg, Germany) and the supplier's software Image Quant 5.2. The time-dependent change of band intensities was fitted by using the program Grafit 3.0 (Erythacus Software Ltd, Staines, UK).

applied successfully to obtain detailed mechanistic insights into the mode of action of biologically active RNA as, for example, natural and artificial antisense RNA<sup>13</sup> or catalytic RNA, including the hammerhead ribozyme.<sup>14</sup>

### Biological activity of two siRNA species against ICAM-1 mRNA

As a model system for this study, we chose the two ICAM-1-directed siRNAs si1 and si2B as well as a 2973 nt long ICAM-1 target RNA that was transcribed *in vitro*. The nucleotide sequence of the ICAM-1 portion of the template plasmid pGEM3Z-ICAM-1 is identical with that of the authentic endogenous ICAM-1 mRNA, except for the very 5' and 3'-portions, which contain plasmid-derived nucleotide sequences. Both siRNAs had been characterized extensively with respect to suppression of the expression of *ICAM-1* in human ECV304 cells. The siRNA si2B was highly active in ECV304 cells at the level of target mRNA and target protein ( $IC_{50}$  0.24 nM), whereas the siRNA si1 was almost inactive ( $IC_{50} > 500$  nM).<sup>12</sup> The sequences of si2B and si1 were chosen such that they share the same GC content, i.e. a comparable thermal stability and that their local target sites are closely positioned within a central segment of the target RNA (Table 1).

### Facilitated strand-exchange between siRNA and its target RNA

Interactions between siRNA and target RNA were measured at physiological ionic strength (100 mM NaCl) and pH (pH 7.4). The temperature was 50 °C and the concentration of CTAB (10 mM) was below the critical micell concentration.<sup>11</sup> RNA strand exchange reactions (Figure 1(A)) were measured by withdrawing aliquots and quenching the reaction with a stop buffer on ice, followed by analysis on polyacrylamide gels under semi-denaturing conditions under which weak intramolecular folding is denatured and duplex RNA of 10–15 bp including siRNA double strands are stable (for experimental details, see Homann *et al.*<sup>9</sup>).

As an apparent product of the strand recognition between siRNA and target RNA, we determined the time-dependent formation of a heteroduplex RNA consisting of the target RNA and the antisense strand of siRNA (termed T·as\*) as well as the decrease of the siRNA (termed s·as\* in Figure 1(B)). Band intensities on gels (Figure 1(B)) were quantified by PhosphorImager analysis, and rate constants were derived as described below and by Homann *et al.*<sup>9</sup> To measure the backward reaction rates, the incubation was started with a heteroduplex RNA formed between the target RNA and the radio-labelled antisense strand of si2B or si1 (Figure 1(C)). All reactions were performed in the presence of CTAB and in the absence of CTAB. However, in the

absence of CTAB, forward reactions were too slow to be measured reliably.

Initial experiments on the concentration-dependence of the strand-exchange of si2B and target RNA suggested that the reaction follows second-order kinetics (data not shown). First, we measured the apparent forward reaction rates in the presence of CTAB, starting with target RNA and siRNA si1 or si2B (Figure 1(B)) under pseudo first-order conditions, i.e. at an excess of target RNA. From those first-order rate constants ( $k^*$ ), the apparent second-order rate constants ( $k_{obs1}$ ) were derived, according to:

$$k_{obs1} = k^*/[\text{target RNA}]$$

Subsequently, we determined the kinetics of the backward reaction ( $k_{obs-1}$ ), i.e. of the interaction between the target-antisense complex (T·as) and the sense strand of siRNA, which gives rise to the re-formation of the siRNA and the release of the target RNA (Figure 1(C)). All rate constants were measured also in the absence of CTAB. However, the forward reactions were too slow to allow reliable values for  $k_{obs1}$  to be derived, whereas values for the backward reaction rate constants ( $k_{obs-1}$ ) were measurable. For this reason, only estimated values for their upper limit can be given, and values for the equilibrium constants  $K_{obs}$  cannot be derived in the absence of CTAB. In this case, the values for  $k_{obs-1}$  are in favor of si2B over si1 by more than 100-fold, which is qualitatively similar to the relative rate constants in the presence of CTAB. These data are summarized in Figure 1(D).

### Recognition of target RNA by siRNA follows an associative mechanism *in vitro*

In principle, the strand-exchange reaction may occur according to either an associative pathway or a dissociative one, as depicted in Figure 2(A). In the case of the situation in living cells, siRNA might either dissociate prior to the binding of its antisense strand to the target or, conversely, a ternary complex may be formed from which the sense strand of the siRNA is released. The following measurements and arguments are consistent with an associative mechanism but not a dissociative one (see Figure 2(A)). The association rate constant for the target (T) and the antisense strand of either si2B or si1 in the absence of CTAB is  $k = 1.2 \times 10^5 \text{ M}^{-1} \text{ s}^{-1}$  and  $k = 0.72 \times 10^5 \text{ M}^{-1} \text{ s}^{-1}$ , respectively (data not shown). Thus, both rate constants are by far too great, and the rates derived thereof are too fast to explain the slow apparent formation of the T·as complex in forward reactions or the reformation of T and as·s for the backward reaction. Further, both rate constants for si2B and si1, respectively, are similar and thus do not explain the substantial difference of the biological activity of both siRNAs. If one assumes that dissociation of as·s was the rate-limiting step of a dissociative pathway, then one

would not assume a dependence of the apparent rates on the concentration of T, neither would one expect the pronounced observed difference of the forward reactions for si2B and si1, respectively, since their calculated thermal stability is very similar (Table 1). Conversely, the concentration-dependence of the overall reaction rates is quite consistent with an associative mechanism. It should be noted that this view cannot be simply applied to the backward reaction. In this case, the RNA structures of the T·as complex for si2B and si1 are likely to differ in the vicinity of the partial duplex, which does not warrant the assumption that this step is similar for both complexes. However, this has no major influence on the biological implications derived from this kinetic study.

### The kinetic of strand displacement is related to the biological activity of siRNA

All forward and backward rate constants for the biologically active siRNA si2B and the inactive species si1 are summarized in Figure 1(D). They show a strong relationship between the biological activity and the kinetics of the interactions with target RNA. The biologically active siRNA si2B shows a 29-fold increased second-order forward rate constant and a 14-fold decreased second-order backward rate constant when compared with the rate constants of the biologically inactive siRNA si1 in the presence of CTAB (Figure 1(D) and Table 1). The apparent equilibrium constant  $K$  is approximately 390-fold in favor of si2B versus si1, for which the  $IC_{50}$  values differ by a factor of equal to or greater than approximately 2000-fold.

To test whether this finding is of a more general relevance, we measured the values of  $k_{obs-1}$  and the efficiency of the forward reaction ( $k_{obs1}$ ) in the presence of CTAB for a larger number of ICAM-1-directed siRNAs, and related these findings to their biological activity against ICAM-1 in human ECV304 cells (Table 1). This relationship is compatible with the more detailed analysis of si1 and si2B (Figure 1(D)). It is noteworthy that si1 and si2B had been designed according to local structural target characteristics rather than parameters intrinsic to the sequences of siRNA.<sup>12</sup> However, the relationship between the kinetics of strand recognition and biological activity is much clearer than that between local target structure and biological activity, which is significant but, on a quantitative basis, less pronounced (data not shown). When testing thermodynamic parameters and sequence characteristics for siRNA that had been related to biological activity,<sup>15</sup> we find only a minor relationship for si1 (zero points) and si2B (four points), though neither score would be considered as favorable. For the other siRNA sequences listed in Table 1, there is no relationship between the scores described by Reynolds *et al.*<sup>15</sup> and their biological activity.

### Implications for the recognition of target RNA by siRNA in living cells

The recognition of target RNA by siRNA in a living cell according to an associative mechanism, i.e. the formation of a ternary complex and a subsequent strand-exchange reaction might have several advantages. Firstly, the RNA–RNA strand-exchange reaction can be promoted by cellular factors to a much greater extent ( $\sim 10^4$ -fold)<sup>9</sup> than RNA–RNA annealing ( $\sim 10^2$ – $10^3$ -fold), which translates into the possibility of a very tight regulation of this process inside cells. Secondly, though speculatively, the strand-exchange reaction might provide a higher target sequence specificity if the cellular machinery that is involved in this process is more sensitive to mis-matched base–base interactions than the system involved in the annealing of two complementary RNA single-strands.

It is important to note that the equilibrium of the strand-exchange reaction is not at the product side for either of the two siRNAs, though for si2B the equilibrium, constant  $K_{obs}$  is less unfavorable (Figure 1(D)). This is consistent with the view that the thermodynamics of the reaction favor exchange when a less folded local target segment is involved (e.g. for si2B) when compared with a thermodynamically more stable local target segment, i.e. a more extensively folded local target structure (e.g. si1). At the biological level, the kinetic model described here does not explain the strong suppression of ICAM-1 gene expression.

For this reason, we postulate a model for the mode of action of siRNA in which a kinetically important step subsequent to the recognition step, maybe associated with the decomposition of the presumed ternary complex (T·as·s) or occurring thereafter (Figure 2(A) and (B)). This presumed step may be sufficiently fast and quasi-irreversible. It might include a nuclease activity that destroys the integrity and thus the biological function of the target RNA, or the release and destruction of the sense strand of the siRNA. It is conceivable that this step includes components of the RISC complex or cellular factors associated with this complex.

According to the model described here, one would assume that siRNA may be bound by RISC and co-factors prior to target recognition. If this complex encounters the target RNA, then strand-exchange may occur. This pathway would not require energy for melting of the siRNA prior to recognition of the target and, thus, it would be favorable in terms of cellular consumption of energy. At the cellular level, saving energy would also make more sense than melting RNA duplexes by a helicase-like activity before this reaction is required.

This kinetic model might be suited to help understand the role of cellular factors and corresponding parameters that determine the biological activity of siRNA. For example, it might be possible that the asymmetric thermal stability of siRNA that

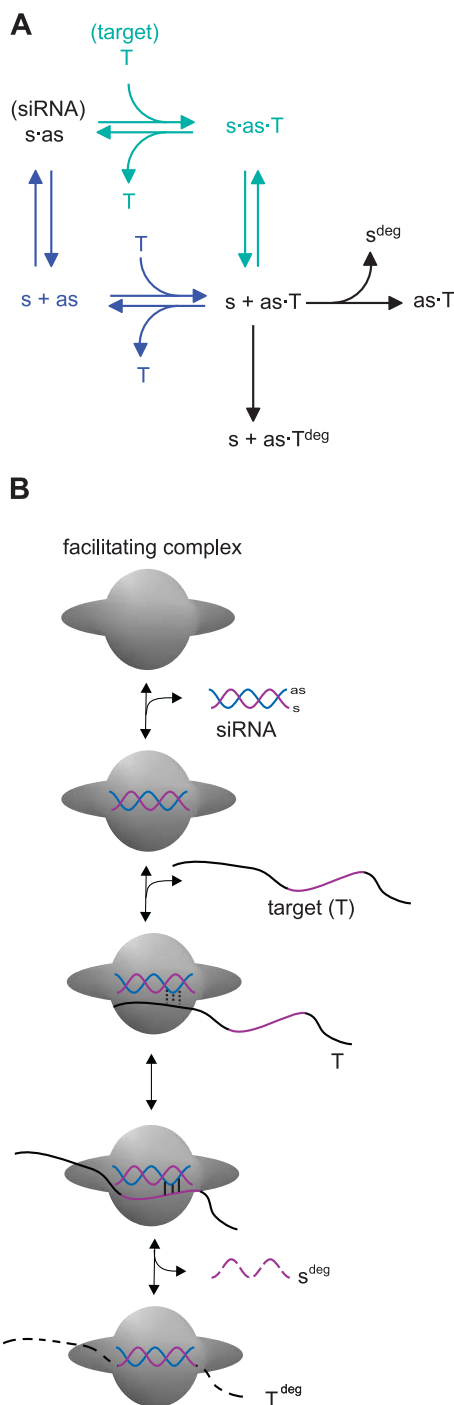


**Figure 2.** A depiction of critical interactions between siRNA and its target. (A) Minimal kinetic scheme describing the apparent strand-exchange between siRNA and target RNA according to a dissociative pathway (blue color) or an associative pathway (green color). The formation of the complex as·T may occur quasi-irreversibly, because either the released sense strand (s) or the target RNA (T) within as·T may become degraded to form biologically inactive products s<sup>deg</sup> or T<sup>deg</sup>, respectively (lower and right panel). (B) A model for the action of siRNA that is consistent with the kinetic data of this study that includes a facilitating complex, which may be part of RISC, or associated with RISC, or related to other factors thought to interact with siRNA. This complex may bind to the siRNA consisting of an antisense

seems to be related to its effectiveness in living cells<sup>1,16</sup> is reflected by the kinetics of siRNA–target interactions *in vitro*. The RNA–RNA strand-exchange reaction described here may further serve as a detection system for cellular factors that are involved in the action of siRNA or its regulation. Such suggested studies may enable one to get new and deeper insights into the mode of action of siRNA in living cells.

## Acknowledgements

We thank Wolfgang Nellen and Marc Lemaitre for fruitful discussions. We thank Rosel Kretschmer-Kazemi Far for kindly providing plasmid pGEM3Z-ICAM-1, Marita Overhoff for preparing figures, and Eurogentec S. A. (Seraing, Belgium) for providing siRNAs.

## References

1. Khvorova, A., Reynolds, A. & Jayasena, S. D. (2003). Functional siRNAs and miRNAs exhibit strand bias. *Cell*, **115**, 209–216.
2. Zhang, H., Kolb, F. A., Brondani, V., Billy, E. & Filipowicz, W. (2002). Human Dicer preferentially cleaves dsRNAs at their termini without a requirement for ATP. *EMBO J.* **21**, 5875–5885.
3. Zamore, P. D., Tuschl, T., Sharp, P. A. & Bartel, D. P. (2000). RNAi: double-stranded RNA directs the ATP-dependent cleavage of mRNA at 21 to 23 nucleotide intervals. *Cell*, **101**, 25–33.
4. Martinez, J., Patkaniowska, A., Urlaub, H., Lührmann, R. & Tuschl, T. (2002). Single-stranded antisense siRNAs guide target RNA cleavage in RNAi. *Cell*, **110**, 563–574.
5. Schwarz, D. S., Hutvagner, G., Du, T., Xu, Z., Aronin, N. & Zamore, P. (2003). Asymmetry in the assembly of the RNAi enzyme complex. *Cell*, **115**, 199–208.
6. Portman, D. S. & Dreyfuss, G. (1994). RNA annealing activities in HeLa nuclei. *EMBO J.* **13**, 213–221.
7. Nedbal, W., Frey, M., Willemann, B., Zentgraf, H.-W. & Sczakiel, G. (1997). Mechanistic insights into p53-promoted RNA–RNA annealing. *J. Mol. Biol.* **266**, 677–687.

(blue color) and a sense strand (margenta) as well as to the target RNA. The sequence portion of the target that is complementary to the siRNA is indicated by margenta color, the non-complementary segments are shown in black color. The facilitating complex is thought to substantially increase the kinetics of subsequent steps of the recognition process, i.e. the formation of a non-specific complex between siRNA and target RNA (three dotted lines), which may dissociate or form a reversible base-specific complex (three continuous lines) in which the sense stand of the siRNA is displaced by the target RNA. Subsequently, a heteroduplex is formed that may be trimmed, leading to degradation products (indicated by dotted lines in black and margenta). This step leads to modified products of the former sense strand (s<sup>deg</sup>) or the target (T<sup>deg</sup>) in a quasi irreversible way.

8. Pontius, B. W. & Berg, P. (1991). Rapid renaturation of complementary DNA strands mediated by cationic detergents: a role for high-probability binding domains in enhancing the kinetics of molecular assembly processes. *Proc. Natl Acad. Sci. USA*, **88**, 8237–8241.
9. Homann, M., Nedbal, W. & Sczakiel, G. (1996). Dissociation of duplex RNA occurs *via* strand displacement *in vitro*: biological implications. *Nucl. Acids Res.* **24**, 4395–4400.
10. Bass, B. L. (2000). Double-stranded RNA as a template for gene silencing. *Cell*, **101**, 235–238.
11. Nedbal, W., Homann, M. & Sczakiel, G. (1997). The association of complementary ribonucleic acids can be greatly increased without lowering the Arrhenius activation energy or significantly altering RNA structure. *Biochemistry*, **36**, 13552–13557.
12. Kretschmer-Kazemi Far, R. & Sczakiel, G. (2003). The activity of siRNA in mammalian cells is related to structural target accessibility: a comparison with antisense oligonucleotides. *Nucl. Acids Res.* **31**, 4417–4424.
13. Wagner, E. G. H. & Simons, R. W. (1994). Antisense RNA control in bacteria, phages, and plasmids. *Annu. Rev. Microbiol.* **48**, 713–742.
14. Hertel, K. J., Herschlag, D. & Uhlenbeck, O. C. (1994). A kinetic and thermodynamic framework for the hammerhead ribozyme reaction. *Biochemistry*, **33**, 3374–3385.
15. Reynolds, A., Leake, D., Boese, Q., Scaringe, S., Marshall, W. & Khvorova, A. (2004). Rational siRNA design for RNA interference. *Nature Biotechnol.* **22**, 326–330.
16. Chiu, Y. L. & Rana, T. M. (2003). siRNA function in RNAi: a chemical modification analysis. *RNA*, **9**, 1034–1048.

*Edited by J. Karn*

*(Received 1 September 2004; received in revised form 14 October 2004; accepted 14 October 2004)*